

# Drilling process monitoring based on operation mode recognition and dynamic feature extraction

Yupeng Li, *Student Member, IEEE*, Weihua Cao, *Member, IEEE*, R. Bhushan Gopaluni, *Member, IEEE*, Wenkai Hu, *Member, IEEE*, Chao Gan, *Member, IEEE*, and Min Wu, *Fellow, IEEE*

**Abstract**—Process monitoring contributes significantly to reducing the risk of downhole faults and preventing undesirable events. This study proposes a process monitoring method based on operation mode recognition and dynamic feature extraction for geological drilling processes. The main idea is to develop different monitoring procedures for various operation modes based on dynamic changes in drilling signals, so as to achieve reliable monitoring for a full drilling cycle including transient and steady-state processes. The contributions are threefold: 1) an operation mode recognition method is developed for drilling processes based on rules discovered from multivariate time series; 2) a long-short term dynamic feature extraction method is proposed to design a process monitoring method for transient processes; 3) a data-driven model based on the long short-term memory is established for time series prediction to monitor steady-state processes. Industrial case studies from a drilling project demonstrate the effectiveness and superiority of the proposed method.

**Index Terms**—Geological drilling, process monitoring, operation mode recognition, dynamic features.

## I. INTRODUCTION

Geological drilling has long been the main way to explore deeply buried natural resources [1]. With the increase in drilling depth, the challenges to drilling safety operations are gradually becoming important. Process monitoring ensures engineering quality and process safety [2], [3]. Generally, drilling process variables are monitored online to ensure signals are within the allowable bounds and the operation is within the safe envelope. However, a drilling cycle is composed of several operation modes [4]. A shift in operation mode causes non-stationarity of the drilling signal; if it is not handled correctly, it can lead to a large number of false alarms and thus reduce trust in the monitoring system. Therefore, a well-designed monitoring system is crucial in reducing the risk of faults and preventing undesirable events that endanger drilling safety.

This work was supported in part by the National Natural Science Foundation of China under Grant 62173313, the 111 project under Grant B17040, and the knowledge Innovation Program of Wuhan-Shuguang Project under Grant 2022010801020208.

Yupeng Li, Weihua Cao, Wenkai Hu, Chao Gan, and Min Wu are with the School of Automation, China University of Geosciences, Wuhan 430074, China, the Hubei Key Laboratory of Advanced Control and Intelligent Automation for Complex Systems, Wuhan 430074, China, and also with the Engineering Research Center of Intelligent Technology for Geo- Exploration, Ministry of Education, Wuhan 430074, China. (e-mail: yupengli@cug.edu.cn; weihuacao@cug.edu.cn; wenkaihu@cug.edu.cn; ganchao@cug.edu.cn; wumin@cug.edu.cn).

R. Bhushan Gopaluni is with the Department of Chemical and Biological Engineering, University of British Columbia, Vancouver, BC V6T 1Z3, Canada. (e-mail: bhushan.gopaluni@ubc.ca).

With the wide application of the data acquisition systems, several advanced data-driven drilling process monitoring methods are proposed and typically derived from the operational data [5], [6]. The main idea of machine learning-based approaches is to learn a latent structure model that can describe the system's normal behavior based on specific information in the data. A large majority of process monitoring methods are based on three typical data representation forms, namely, original samples, their probability distribution, and time series.

A common way to ensure drilling safety is by monitoring the original samples. Some advanced drilling systems were equipped with alarm configuration modules to make monitoring decisions by checking whether the samples exceeded a pre-defined limit. However, the limit setting depends on the operator's prior experience and is often subjective [7]. Regarding monitoring methods, the principal component analysis was used to extract latent variables related to the stuck fault [8]. Neural networks were used to diagnose downhole faults with online collected samples as the input [9]. However, these methods are challenging to capture the dynamic features of drilling signals, so they are only applicable at steady-state.

The probability distribution is an essential tool to describe the shape of a dataset [10], [11]. It is possible to conduct drilling process monitoring by detecting changes in data distribution. The generalized likelihood tests and multivariate t-distribution were combined to make efficient washout detection [12]. Considering the limited faulty drilling data, the difference between standard reference and online data distribution is calculated to monitor drilling safety. The Kullback-Leibler divergence was used as a dissimilarity index to detect bit bounce faults [13]. Although this kind of method shows advantages in incipient fault detection, it is difficult to monitor the dynamic properties of drilling signals without considering time series dependencies.

Typical approaches for analyzing drilling time series include trend analysis and distance calculations [14]. The presence of faults can change the dependencies of the time series; this makes the trend features of drilling signals important information for process monitoring [15]. For instance, a downhole fault detection algorithm was developed based on global trend and local trend extraction [16]. Abnormal trends in drilling time series were extracted based on reconstruction analysis and time series segmentation methods [17]. The fracturing pressure time series was modeled by locally weighted linear regression to develop an early warning model [18]. Further, if the relationship from derivatives to faults is not straightforward, they can be transformed into a set of symbols

relating to trend features. Symbolic time series were used to build a downhole fault diagnosis model [19]. Besides trend features, distance calculation between time series is another idea for drilling fault detection. First, calculating the labeled time series templates corresponding to certain conditions in advance; then, determining the state by measuring the distance between the target signal and templates. The kick probability was calculated by a similarity measure algorithm based on the Euclidean distance and pattern recognition model [20]. A diagnostic decision was made using dynamic time warping and density-based clustering [21]. Nevertheless, the distance-based machine learning method fails to detect faults effectively and timely since it requires a longer time series in a fault state.

According to the above literature survey, existing methods have limitations in their design for drilling process monitoring. On the one hand, most methods designed for fault detection focus on the steady-state of the process, regardless of other transient operation processes in a drilling cycle. On the other hand, the drilling signal changes dynamically due to the formation uncertainty; existing methods fall short of fully capturing the time series dependencies. Motivated by the above challenges, this paper proposes a systematic drilling process monitoring method based on operation mode recognition and dynamic feature extraction. The main contributions of the proposed method are threefold: 1) an operation mode recognition method is developed for drilling processes based on rules discovered from multivariate time series; 2) a long-short term dynamic feature extraction method is proposed to design a process monitoring method for transient processes; 3) a data-driven model based on long short-term memory is established for time series prediction to monitor steady-state processes. Case studies with actual drilling data are provided to illustrate the practical effectiveness of the method.

The remainder of this paper is organized as follows: The problem is formulated in Section II. The proposed monitoring methodology is presented in Section III. Case studies are given in Section IV, followed by conclusions in Section V.

## II. PROBLEM FORMULATION

A geological drilling process consists of three main systems, namely, rotary system, hosting system, and hydraulic system. The main function of the first two systems is to provide power to break downhole rocks. The schematic of the hydraulic system is shown in Fig. 1, where a mud pump delivers the mud fluid from a mud pit to the drill bit through a drillstring, and then the mud returns to the surface from the annulus between the drillstring and formation.

In a drilling process, a mud pump delivers the mud fluid from a mud pit to the drill bit through a drillstring, and then the mud returns to the surface from the annulus between the drillstring and formation [13]. The flowing mud removes downhole broken stones to improve efficiency, while the mud column provides hydrostatic pressure to balance formation pressures, preventing wall collapse, lost circulation, and kick incidents. The standpipe pressure (SPP) is the sum of pressure drops in the mud cycle circuit; and the mud flow in (MFI) is defined as the mud flow rate into the well. In practice, drilling

operators monitor the drilling condition mainly by observing the changes in the key variable SPP, and the adjustment of the operational variable MFI directly affects the monitoring variable SPP.

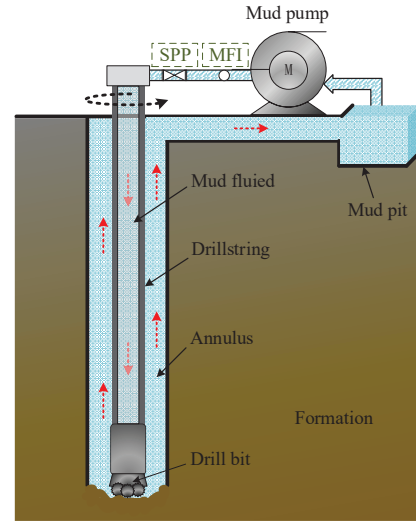


Fig. 1. Schematic of the hydraulic system in a drilling process. The red arrows represent the directions of mud fluid flows. The process variables SPP and MFI are displayed on dashed green rectangles.

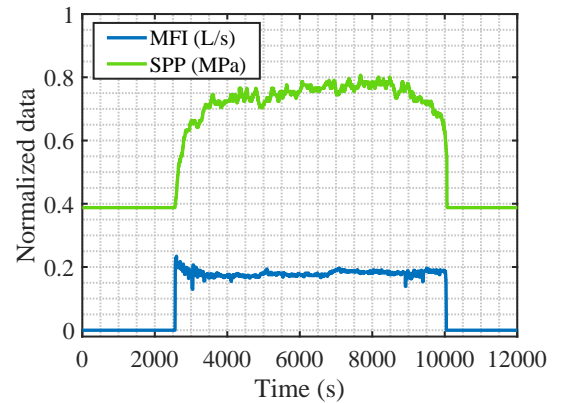


Fig. 2. Normalized SPP and MFI signals in a drilling cycle including transient and steady-state operation modes in the normal state.

The SPP and MFI signals reflect the safety of the hydraulic system. The SPP signal typically fluctuates in a small range in the normal state configured with a constant MFI setpoint. However, this relationship does not hold when a fault occurs. Notably, the MFI setpoint is adjusted during the start-up and shut-down operations, thereby leading to the non-stationarity of the SPP signal. Drilling signals exhibit different dynamic information in normal, start-up, and shut-down operations. For example, Fig. 2 shows the MFI and SPP signals in a typical drilling cycle. The MFI signal rose sharply at  $t = 2500$  and dropped discernibly at  $t = 10000$ . Meanwhile, the SPP signal showed an upward trend during the start-up process within  $t \in (2500, 4000)$ , and exhibited a downward trend in the shut-down process within  $t \in (9000, 10000)$ . By contrast, the SPP signal fluctuated smoothly during the steady-state mode

between start-up and shut-down. This leads to the development of different monitoring methods based on the dynamic features of signals in various operation modes.

As shown in Fig. 2, the dynamic changes of the MFI and SPP signals are sensitive to the operation mode, so discovering the rules related to dynamic changes is critical for mode recognition. Thus, this study is motivated by human experiences and aims to propose a data-driven method to conduct drilling process monitoring based on the key variables SPP and MFI. Drilling operation modes are divided into transient and steady-state modes; typical transient operation modes occur during the start-up and shut-down processes, and the steady-state mode corresponds to the stable drilling process between the start-up and shut-down.

### III. THE PROPOSED METHOD

This section presents the drilling process monitoring method. Fig. 3 shows the framework of the method. The drilling process data include time series of SPP and MFI. First, the drilling operation mode is recognized based on symbolic aggregate approximation (SAX) and association rules. Then, the long-short term dynamic features are extracted for the transient process monitoring; and a time series prediction model based on long short-term memory (LSTM) is established for the steady-state process monitoring.

#### A. Operation mode recognition

Considering that the drilling process is dynamic, the information associated with operation modes is reflected in the signal variations instead of the original value [22]. The key problem is to extract the trends of multiple drilling signals accurately. Then, the trends extracted at each moment constitute a continuous sequence of events. Further, another problem is to establish the relationship between the event sequences and the drilling operational mode based on association rules, which can be extracted from historical data.

The drilling time series composed of continuous numerical values is difficult to describe by rules related to the operation mode. To solve the problem, the first step is to discretize the time series and represent it with a set of symbols. Time series representation not only reduces computational complexity, but also discovers the trends of change and associates them with rules. Here, SAX converts the time series into a set of customizable symbols. The main idea is to divide the time series into several segments with a sliding window and assign a symbol to each point to represent the current variational direction.

The time series of the original SPP and MFI are represented by  $x_s^o$  and  $x_m^o$ , respectively. First, the original data  $x_s^o$  and  $x_m^o$  are normalized as

$$x_v(t) = \frac{x_v^o(t) - x_{v,min}^o}{x_{v,max}^o - x_{v,min}^o}, \quad (1)$$

where  $v \in \{s, m\}$ ,  $t$  denotes the time stamp,  $x_{v,min}^o$  and  $x_{v,max}^o$  represent the minimum and the maximum values in  $x_v^o$ , respectively.

To preserve the dynamic information of  $x_v(t)$ , a local linear regression model is used to fit  $x_v$  as

$$x_v(t) = p_v(k)t + q_v(k), t \in [k+1-w, k], \quad (2)$$

where  $p_v(k)$  represents the slope parameter,  $q_v(k)$  denotes the intercept parameter, and  $w$  is considered as the sliding window length. The estimated values of  $p_v(k)$  and  $q_v(k)$  are obtained by minimizing the error as follow,

$$(\hat{p}_v(k), \hat{q}_v(k)) = \operatorname{argmin}_{t=k+1-w}^k (x_v(t) - p_v(k)t - q_v(k)), \quad (3)$$

then, the analytic form of the estimated value is

$$\hat{p}_v(k) = \frac{\sum_{t=k+1-w}^k (x_v(t) - \bar{x}_v(k))(t - \bar{t})}{\sum_{t=k+1-w}^k (t - \bar{t})^2}, \quad (4)$$

where  $\bar{x}_v(k)$  and  $\bar{t}$  are the mean values of  $x_v(t)$  and  $t$  in the interval  $t \in [k+1-w, k]$ .

Next, the  $\hat{p}_v$  is converted into a set of symbols to describe the variational direction; here, every element  $\hat{p}_v(k)$  is mapped to one of the discrete intervals with a certain symbol, i.e.,

$$c_v(k) = \begin{cases} 0 & l_v \leq \hat{p}_v(k) \leq u_v \\ -1 & \hat{p}_v(k) < l_v \\ 1 & u_v < \hat{p}_v(k) \end{cases} \quad (5)$$

where the symbols 0, -1, and 1 represent stable, downward, and upward trends, respectively;  $l_v$  and  $u_v$  denote the lower and upper bounds for  $\hat{p}_v(k)$ , respectively. The bounds are calculated based on three-sigma limits for the estimated Gaussian distribution of normal historical data [23].

In drilling processes, measurement noises and downhole interference are inevitable. This leads to introducing the delay timer in alarm management to avoid repeated changes in  $c_v(k)$  caused by signal fluctuations [24]. Specifically, if  $c_v(k)=\alpha$ ,  $c_v(k+\tau_v)$  changes to  $\beta$  ( $\alpha \neq \beta$ ) only when all elements in  $\{\hat{p}_v(i) | i = k, k+1, \dots, k+\tau_v\}$  satisfy the conditions corresponding to  $\beta$  in eq. (5), where  $\tau_v$  is a delay parameter; otherwise, the value of  $c_v$  does not change, i.e.  $c_v(k+\tau_v)=\alpha$ .

In the steady-state mode, the variational direction of the drilling signal rarely changes. By contrast, transient operations always accompany changes in variational directions. It is possible to discover the time series segments that the co-occurrence of changes in variational directions of SPP and MFI signals; then, the association rules related to these segments are extracted from the historical data to recognize the transient mode.

A symbolic segment of multiple adjacent variational directions is regarded as an event. For example, during the start-up process, MFI rises first, and SPP climbs up later. This can be formulated as a rule that an increase in SPP (event  $A$ ) is followed by a rise in MFI (event  $B$ ). The event  $A$  describes the transition of the variational direction of MFI from stable ( $c_m = 0$ ) to upward ( $c_m = 1$ ), i.e.  $[0,0,1,1]$ ; while the event  $B$  expresses that  $c_s$  shifts from 0 to 1, i.e.  $[0,0,1,1]$ . The association rule from event  $A$  to event  $B$  is denoted as  $A \rightarrow B$ . By combining the variational direction vectors corresponding

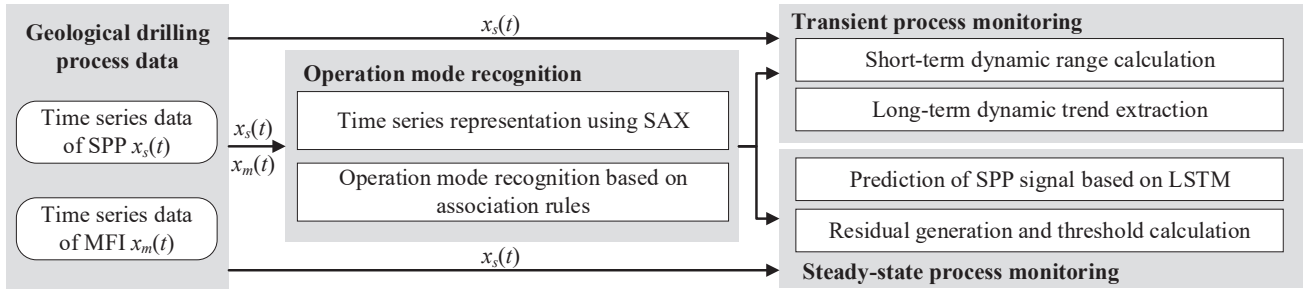


Fig. 3. A framework of the proposed process monitoring method for geological drilling.

to  $A$  and  $B$ , a reference matrix  $C_{A \rightarrow B}$  representing the rule  $A \rightarrow B$  is given as follow:

$$C_{A \rightarrow B} = \begin{pmatrix} 0 & 0 & 1 & 1 & 1 \\ 0 & 0 & 0 & 1 & 1 \end{pmatrix}. \quad (6)$$

The rows of  $C$  correspond to drilling variables; the columns are samples of variational directions. Then, the reference matrix corresponding to each operation mode is prepared for online mode recognition.

### B. Transient process monitoring using dynamic features

This section proposes a transient process monitoring method based on long-short term features of the SPP signal, so as to prevent false alarms due to shifts in operation modes and ensure the safety of transient processes of the mud pump.

1) *Short-term monitoring with a dynamic range*: The goal of the short-term monitoring is to determine whether the SPP signal  $x_s$  changes significantly in a small interval. To detect abrupt rises or falls of  $x_s$  signal, the relative difference between two adjacent samples is calculated as the short-term dynamic feature and monitored in a step-by-step manner. The dynamic range  $\theta(k)$  for  $x_s(k)$  is designed based on the previous sample  $x_s(k-1)$  and the limits for the slope parameter  $p_s$  in eq. (4). The historical data under the transient process is used to calculate the maximum limit  $p_s^{max}$  and the minimum limit  $p_s^{min}$  for the slope parameter  $p_s$ , where the boundaries are determined using three-sigma limits.

The range  $\theta(k)$  is calculated based on the local linear regression model. First, boundaries  $q_s^{max}(k)$  and  $q_s^{min}(k)$  of the intercepts correspond to  $p_s^{max}$  and  $p_s^{min}$  at  $k$  are given by:

$$q_s^{max}(k) = x_s(k-1) - p_s^{max} * (k-1), \quad (7)$$

$$q_s^{min}(k) = x_s(k-1) - p_s^{min} * (k-1). \quad (8)$$

Then, the upper and lower limits of  $x_s(k)$  are calculated as:

$$x_s^{max}(k) = p_s^{max} * k + q_s^{max}(k), \quad (9)$$

$$x_s^{min}(k) = p_s^{min} * k + q_s^{min}(k). \quad (10)$$

Last, the dynamic range  $\theta(k)=[x_s^{min}(k), x_s^{max}(k)]$  for  $x_s(k)$  is established for short-term monitoring.

However, the dynamic range can only monitor the change of  $x_s$  in a short-term. Since the  $p_s^{max}$  and  $p_s^{min}$  represent the extreme cases of slope values, even if  $x_s(k) \in \theta(k)$ , the system may deviate from the normal state. For example, the

$x_s$  should continue to increase during the start-up process, but  $p_s^{min}$  may be negative due to signal fluctuations; if  $x_s$  keeps slowly decreasing, such an undesirable event is difficult to discover due to  $p_s > p_s^{min}$ . To address this problem, the long-term dynamic feature is introduced to monitor the trend of  $x_s$ .

2) *Long-term monitoring based on dynamic trend extraction*: During the start-up and shut-down processes, the trend information of the signal plays a vital role in safety monitoring. The Mann-Kendall (MK) test showed outstanding performance in the trend extraction of time series in industrial processes [25]. The MK test is a nonparametric test designed to statistically calculate a signal's increasing or decreasing trend over time. Compared with the short-term monitoring that only models the one-step change, the MK test can capture a long-term dependency, and thus is introduced to calculate the long-term dynamic feature of  $x_s$ .

The observations of  $x_s$  obtained over time form a time series  $[x_s(k-n+1), \dots, x_s(k-1), x_s(k)]$ , where  $n$  denotes the number of observations. Under the assumption that each observation is independent and identically distributed, the MK summation  $M$  is defined to compare observations obtained earlier and those obtained later, that is,

$$M(k) = \sum_{j=k-n+1}^{k-1} \sum_{i=j+1}^k \text{sign}(x_s(i) - x_s(j)), \quad (11)$$

where  $\text{sign}(\cdot)$  denotes a symbolic function determined by the sign of  $x_s(i) - x_s(j)$  as

$$\text{sign}(x_s(i) - x_s(j)) = \begin{cases} 1 & x_s(i) - x_s(j) > 0 \\ 0 & x_s(i) - x_s(j) = 0 \\ -1 & x_s(i) - x_s(j) < 0 \end{cases}. \quad (12)$$

If the number of observations is sufficient ( $n > 10$ ), the test is conducted by calculating the variance  $V_M$  and the MK statistic  $Z$  as follows [25]

$$V_M(k) = \frac{n(n-1)(2n+5)}{18}, \quad (13)$$

$$Z(k) = \begin{cases} \frac{M(k)-1}{\sqrt{V_M(k)}} & M(k) > 0 \\ 0 & M(k) = 0 \\ \frac{M(k)+1}{\sqrt{V_M(k)}} & M(k) < 0 \end{cases}. \quad (14)$$

The sign of  $Z(k)$  is related to the trend of  $x_s$  over time, and the absolute value of  $Z(k)$  is associated with the degree of

change of  $x_s$  in the interval  $t \in [k - n + 1, k]$ . If  $Z(k) > 0$ , it indicates that the  $x_s$  shows an upward trend; if  $Z(k) < 0$ , it means that the  $x_s$  exhibits a downward trend.

According to expert rules and drilling knowledge, the reference directions of change of SPP under normal transient processes can be summarized as follows: the SPP signal should increase (i.e.,  $Z(k) > 0$ ) in the start-up process and decrease (i.e.,  $Z(k) < 0$ ) in the shut-down process.

### C. Steady-state process monitoring via time series prediction

The monitoring of the steady-state process mainly includes two parts: the SPP signal is predicted based on a prediction model, and then a residual signal is generated and compared with a pre-calculated threshold to detect potential faults.

1) *Prediction of SPP signal based on LSTM network:* In an actual drilling process, the time-varying SPP signal is related to both the current condition and the previous moments. This leads to the SPP signal showing both long-term and short-term dynamic characteristics. For example, kick and loss faults often cause slow varying changes in the SPP signal, while the failure of broken tools usually leads to abrupt changes in the SPP signal. Recently, many studies found that Long Short-Term Memory (LSTM) is useful in time series modeling tasks. Adopting the LSTM network to predict SPP can compensate for the weakness of using only the information within the sliding window, and thus it is used to build the prediction model.

Fig. 4 shows the architecture of the prediction model based on the LSTM network. For online collected SPP samples, the information flow into the LSTM is controlled by three gates: a forget gate, an input gate, and an output gate; in addition to the current input, the output also depends on the cell state associated with historical inputs.

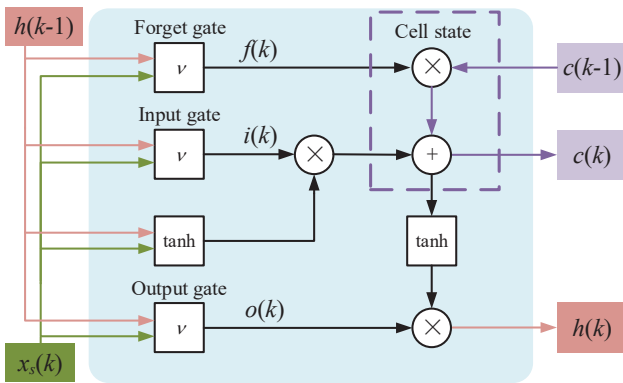


Fig. 4. Architecture of LSTM-based SPP prediction model.

The SPP sample and hidden state at the current time stamp  $k$  are  $x_s(k)$  and  $h(k-1)$ , respectively. A part of the information in cell state  $c(k-1)$  at the previous moment is removed from the cell  $c(k)$  by the forget gate  $f(k)$  as

$$f(k) = \nu(W_f x_s(k) + U_f h(k-1) + b_f), \quad (15)$$

where  $\nu$  denotes a control function,  $W_f$  and  $U_f$  are weight parameters, and  $b_f$  is the bias parameter. In the following

eqs. (16-19),  $\{W_i, W_o, W_c\}$  and  $\{U_i, U_o, U_c\}$  indicates weight parameters, and  $\{b_i, b_o, b_c\}$  are bias parameters.

To determine which information in  $x_s(k)$  and  $h(k-1)$  should be passed to cell  $c(k)$ , the input gate  $i(k)$  is designed to control the effect of the input as

$$i(k) = \nu(W_i x_s(k) + U_i h(k-1) + b_i). \quad (16)$$

Based on  $f(k)$  and  $i(k)$ , the information contained in the cell  $c(k-1)$  is partially forgotten, then the cell is updated via the following procedure

$$c(k) = f(k) \star c(k-1) + i(k) \tanh(W_c x_s(k) + U_c h(k-1) + b_c), \quad (17)$$

where  $\star$  represents an element-wise product function. Here, the range of  $f(k)$  is  $[0, 1]$ ; if  $f(k)$  approaches 0, the historical information is almost completely forgotten. On the contrary, all historical information is preserved.

Then, the output  $h(k)$  of the LSTM model is determined by the output gate  $o(k)$  and the cell state  $c(k)$ :

$$o(k) = \nu(W_o x_s(k) + U_o h(k-1) + b_o), \quad (18)$$

$$h(k) = o(k) \star \tanh(c(k)), \quad (19)$$

where  $h(k)$  is equal to the predicted SPP signal  $\hat{x}_s(k+1)$ .

In the training process, the weights  $W$  and  $U$ , and bias  $b$  in eqs. (15-19) are determined based on historical drilling data. Then, the SPP signal is predicted online based on the trained LSTM network.

2) *Residual signal generation and threshold calculation:* Residual signal generation and threshold calculation are the two key steps to determine whether the drilling system has deviated from the normal state. First, the predicted future SPP signal  $\hat{x}_s$  and the measured SPP signal  $x_s$  are fed into a residual generation model. Then, the generated residual signal  $r(k)$  is compared with a pre-defined threshold  $\gamma$  determined from historical data in the normal state to make a decision.

The residual  $r(k)$  is generated by calculating the absolute difference of the predicted and measured signals as

$$r(k) = |\hat{x}_s(k) - x_s(k)|. \quad (20)$$

Further, the drilling process monitoring following the residual signal discrimination can be formulated as a hypothesis-testing problem:

$$\begin{cases} H_0 : x_s(k) \text{ is in a normal state,} \\ H_1 : x_s(k) \text{ is in an abnormal state,} \end{cases} \quad (21)$$

where the null hypothesis  $H_0$  indicates that the system is in the normal state, and the alternative hypothesis  $H_1$  indicates that the system is in an abnormal state.

If  $r(k)$  exceeds a threshold for the normal state, it implies that the system deteriorated into an abnormal state. Further, the decision rule for the hypothesis-testing problem in eq. (21) is rewritten as

$$\begin{cases} \text{Decide on } H_0 \text{ when } r(k) \leq \gamma, \\ \text{Decide on } H_1 \text{ when } r(k) > \gamma, \end{cases} \quad (22)$$

where  $\gamma$  represents a pre-defined threshold determined from  $r(k)$  in the normal state, and the threshold is calculated based on the three-sigma rule.

Assume that the residuals corresponding to the historical SPP data in steady-state processes are denoted as  $\Theta = [r_s(1), r_s(2), \dots, r_s(N)]$ , where  $N$  is the number of elements. The estimated probability density function  $\hat{g}(r)$  of  $\Theta$  is obtained using the kernel density estimation as

$$\hat{g}(r) = \frac{1}{Nb} \sum_{i=j}^N \mathcal{K}\left(\frac{r - r_s(j)}{b}\right), \quad (23)$$

where  $\mathcal{K}(\cdot)$  is the Gaussian kernel function,  $r_s(j)$  represents the  $j$ th element in  $\Theta$ , and the bandwidth  $b$  is determined by a general formula as [13]

$$b = \left(\frac{4\sigma_s^5}{3N}\right)^{\frac{1}{5}}, \quad (24)$$

where  $\sigma_s$  denotes the variance of  $r_s$ . Next, the threshold  $\gamma$  under a confidence level  $\alpha$  is calculated as follow:

$$\mathcal{P}(r \leq \gamma) = \int_0^{\gamma} \hat{g}(r) dr = \alpha. \quad (25)$$

#### D. Summary of the proposed method

The online monitoring procedure is summarized in Algorithm 1. The input is the data collected online. The output is the alarm state, i.e., normal ( $alarm = 0$ ) or faulty ( $alarm = 1$ ), where the default value of  $alarm$  is 0. The steady-state mode, start-up mode, and shut-down mode are respectively denoted as  $\rho_s$ ,  $\rho_u$ , and  $\rho_o$ , and reference matrices corresponding to these modes are respectively expressed as  $C_s$ ,  $C_u$ , and  $C_o$ . The operation mode at  $k$  is denoted as  $\rho_c(k)$ .

**Remark 1.** This study is motivated by drilling signals showing different variation characteristics in drilling operation modes. Compared with the existing work, the proposed method is novel in the following aspects: 1) the proposed method determines drilling operation modes prior to process monitoring, which does not exist in any literature [8], [16]; 2) short-term dynamic alarm ranges are designed for transition process monitoring, where many existing methods are based on fixed or adaptive thresholds [1], [13]; 3) the proposed method introduces a time series prediction model with long-term memory for steady-state process monitoring, whereas the sequence dependencies are not considered by most existing methods [21].

## IV. CASE STUDY

This study provides an industrial case study with data from a geological drilling site in Jiaodong Peninsula, China. The effectiveness of the proposed method is verified in terms of operation mode recognition, transient process monitoring, and steady-state process monitoring. The dataset consists of MFI and SPP data from depths of 2477 to 2930 meters with a sampling interval of 1 second. The training dataset consists of 60,000 historical samples of multiple segments under normal drilling conditions.

---

### Algorithm 1 Online monitoring for the drilling process.

---

```

Input: Data collected online;
Output: Alarm states;
while data samples are updated at  $k$  do
    Sliding the window to  $t \in [k + 1 - w, k]$ ;
    Calculate  $p_v(k)$  and  $c_v(k)$  using eqs. (4-5);
    Create the matrix  $C$  with  $\mathbf{c}_m$  and  $\mathbf{c}_s$ ;
    if  $C = C_g, C_g \in \{C_s, C_u, C_o\}$  then
         $\rho_c(k) = \rho_g, \rho_g \in \{\rho_s, \rho_u, \rho_o\}$ ;
    else
         $\rho_c(k) = \rho_c(k - 1)$ ;
    end if
    if  $\rho_c(k) = \rho_s$  then
        Predict  $\hat{x}_s(k)$  using the LSTM-based model;
        Calculate  $r(k)$  using eq. (20);
        if  $r(k) > \gamma$  then
            return  $alarm=1$ ;
        end if
    else
        Calculate  $\theta(k)$  using eqs. (7-10);
        if  $x_s(k) \notin \theta(k)$  then
            return  $alarm=1$ ;
        else
            Calculate  $Z(k)$  using eq. (14);
            if  $\rho_c(k) = \rho_u$  and  $Z(k) \leq 0$  then
                return  $alarm=1$ ;
            else
                if  $\rho_c(k) = \rho_o$  and  $Z(k) \geq 0$  then
                    return  $alarm=1$ ;
                end if
            end if
        end if
    end if
end while
    
```

---

#### A. Operating mode recognition

According to the method in Section III-A, the historical time series of MFI and SPP were segmented by sliding windows with  $w=60$  and converted to symbols  $\{0, -1, 1\}$ . The delay parameters for SPP and MFI are  $\tau_s = 10$  and  $\tau_m = 10$ . Table I summarizes the association rules discovered from historical data for recognizing drilling modes. For example, the rule for the start-up mode is that the SPP signal rises following the rise of the MFI signal from zero. The above two events are described using  $\mathbf{c}_m = [0, 0, 1, 1]$  and  $\mathbf{c}_s = [0, 0, 1, 1]$ . According to Table I, a switch label  $c_l$  indicating the co-occurrence of the exact variational directions in  $c_m$  and  $c_s$  is defined as

$$c_l(k) = \begin{cases} 1 & \text{Start-up} \\ -1 & \text{Shut-down} \\ 0 & \text{Steady-state} \end{cases}, \quad (26)$$

where a positive  $c_l(k)$  represents the start of the start-up mode, and a negative represents the start of the shut-down mode.

Using the association rules in Table I, the mode recognition results covering three drilling cycles are shown in Fig. 5, where the blue curve denotes the MFI signal, the green curve

TABLE I  
ASSOCIATION RULES FOR DRILLING OPERATION MODE RECOGNITION.

Pattern	$c_m$	$\rightarrow$	$c_s$
Start-up mode	[0, 0, 1, 1]	$\rightarrow$	[0, 0, 1, 1]
Shut-down mode	[0, 0, -1, -1]	$\rightarrow$	[0, 0, -1, -1]
Steady-state mode		Otherwise	

represents the SPP signal, the blue and green stars indicate the variational directions  $c_m$  and  $c_s$ , respectively, and the red stars represent the switch label  $c_l$ . The three start-up and shut-down modes were successfully recognized using  $c_l$ , and other moments were correctly recognized as the steady-state mode.

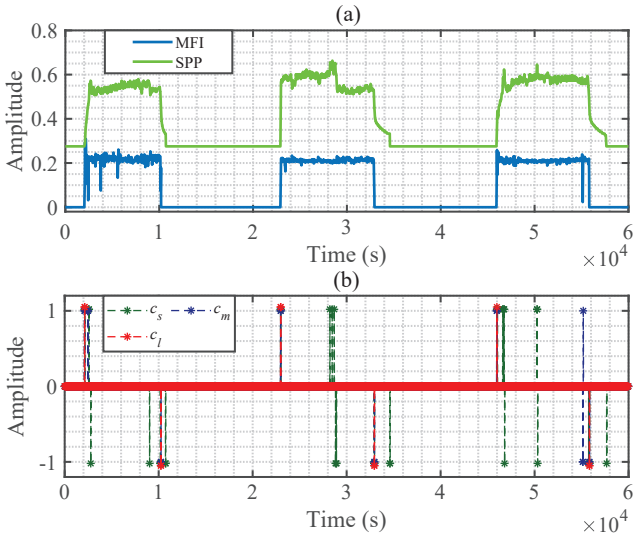


Fig. 5. Time series plots of process signals for three drilling cycles, where the blue curve denotes the MFI signal, the green curve represents the SPP signal, the blue and green stars indicate the dynamic features  $c_m$  and  $c_s$ , respectively, and the red stars represent the switch label  $c_l$ .

To show the recognition process more clearly, Fig. 6 only shows time series of process signals during a single start-up process in Fig. 5. First, an upward trend in MFI was captured and then caused  $c_m$  to change from zero to positive. Then,  $c_s$  went from zero to positive after detecting a rise in SPP. Changes in  $c_m$  and  $c_s$  caused the switch label  $c_l$  to become positive, indicating that the system shifted to the start-up mode at  $t = 45990$ , so the start-up mode was correctly recognized.

### B. Transient process monitoring

After the transient operation mode is recognized, it is necessary to monitor the dynamic change of the SPP signal. Fig. 7 shows the time series plot of SPP and the corresponding long-short term dynamic features in two start-up cases. The blue curves denote SPP signals; the dashed red and yellow curves indicate upper and lower limits, respectively, which were calculated at the 95% significance level based on historical data for start-up processes. In Figs. 7(a) and (c), the SPP signal was within the upper and lower limits, and the MK statistics  $Z$  kept rising, indicating that the long-term trend for SPP was upward, which was consistent with the rule for the

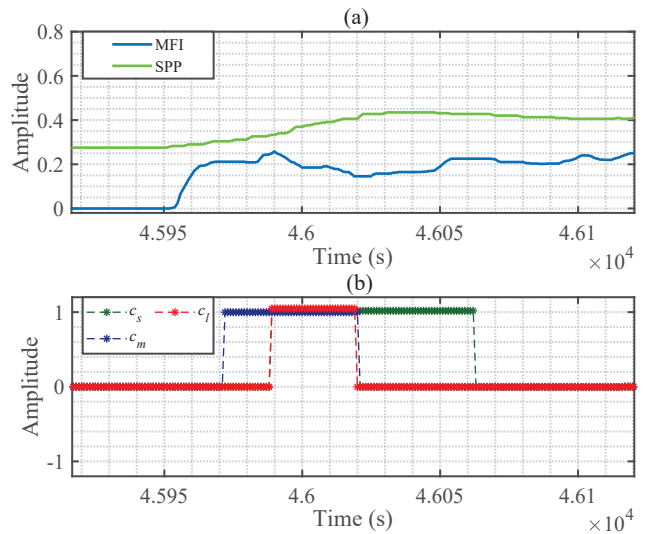


Fig. 6. Time series plots of process signals for a start-up process.

normal start-up mode. In Figs. 7(b) and (d), an abnormal event occurred at  $t = 270s$ , causing the SPP signal that should be rising to drop. The abnormal interval is highlighted with red backgrounds; the SPP signal exceeded the dynamic range, and the MK indicator  $Z$  dropped. The long-short term dynamic features indicated that the system was abnormal.

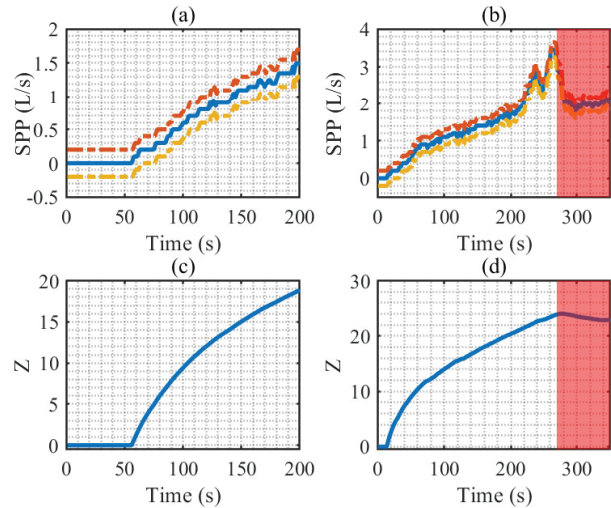


Fig. 7. Time series plots of SPP and the corresponding dynamic features for two start-up cases. In (a) and (b), the blue curves denote the SPP signal, the dashed red and yellow curves represent the upper and lower limits, respectively. In (c) and (d), the blue curves show the MK statistics.

Figs. 8(a) and (b) show the time series plots of SPP and the corresponding dynamic ranges in two shut-down cases. It can be seen that the SPP signals denoted by blue curves were always in the intervals between the upper and lower limits. The long-term dynamic trend of SPP for the shut-down mode is the opposite of that of the start-up mode. In Figs. 8(c) and (d), the MK statistics  $Z$  in both cases were negative, expressing that SPP signals showed long-term downward trends, which matched the rule for the shut-down mode. The above results illustrate the effectiveness of the long-short term dynamic

feature for transient process monitoring.

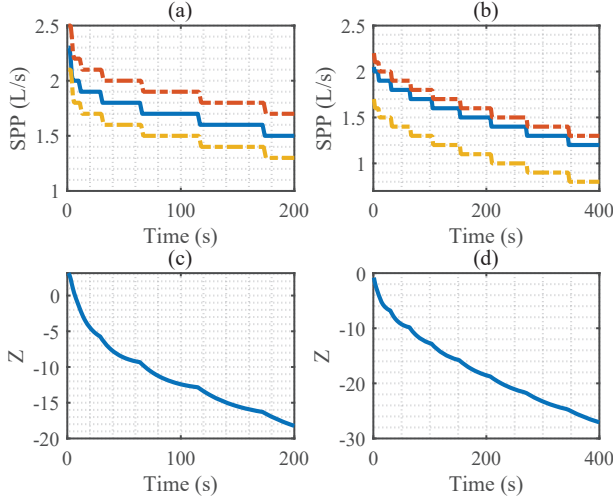


Fig. 8. Time series plot of SPP and corresponding long-short term dynamic features in two shut-down cases.

### C. Steady-state process monitoring

The steady-state mode accounts for most of the drilling time. Fig. 9 shows the time series plots for SPP and its residual signals. The LSTM model was trained on 30,000 samples of normal operations. In Fig. 9 (a), the blue solid curve and red dashed curve denote the original and predicted signals, respectively. The residual signal generated by the difference between the above two signals is shown in Fig. 9 (b), where the red background indicates the abnormal conditions, and the red dashed line denotes the alarm threshold. A downhole abnormal event caused significant changes in the SPP signal in  $t \in [2700, 2900]$ , resulting in the residual signal rising sharply and violating the threshold. After that, the signal also showed an abnormal rise at  $t = 3700s$ , and the abnormality lasted about 100 seconds. Then, the operator found the abnormality and adjusted other drilling parameters. Obviously, these abnormal events were successfully detected with the significant rise of the residual signal. Apart from these events, the residual signal was almost always below the threshold, indicating that the system was in a normal state.

To demonstrate the superiority of the method to other methods, monitoring results using different methods in the steady-state operation mode are shown in Table II. The false alarm rate (FAR) and missed alarm rate (MAR) are used as indicators to evaluate monitoring performance [26]. The FAR and MAR of the proposed method were 0.77% and 1.06%. The results of the back-propagation neural network (BPNN) were worse than those of the other three methods. Compared with the principal component analysis (PCA) and autoencoder, the proposed method showed a lower FAR when the MARs were similar. Therefore, the performance of the proposed method outperformed the other three methods.

## V. CONCLUSION

This paper proposes a process monitoring method based on operation mode recognition and dynamic feature extraction for

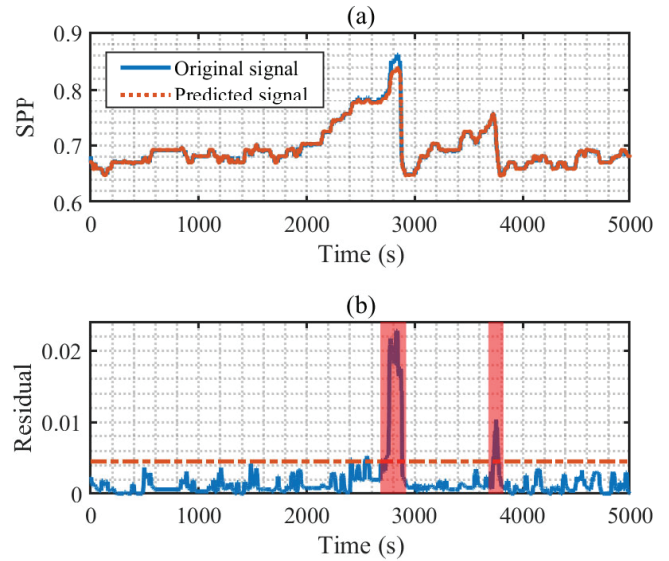


Fig. 9. Time series plots of SPP and residual signals; (a) the blue solid curve and red dashed curve denote the original signal and the predicted signal, respectively; (b) the blue solid curve denotes the residual signal, and the red dashed line represents the alarm threshold.

TABLE II  
COMPARISON OF MONITORING RESULTS USING DIFFERENT METHODS.

Method	FAR (%)	MAR (%)
$T^2$ of PCA	10.07	1.95
BPNN	9.80	3.57
Autoencoder	9.71	1.96
The proposed method	1.02	2.12

the geological drilling process. Association rules related to the drilling operation mode are discovered based on variational directions, and then the operation mode is recognized with the association rules. For the transient mode, a time-varying dynamic range is designed to monitor the SPP in the short-term; the long-term dynamic trend is extracted to calculate the direction of change. For the steady-state mode, a residual signal is generated using the future SPP signal predicted by the prediction model; then, a monitoring decision is made by comparing the residual signal with a pre-defined threshold. Case studies involving the data collected from a drilling project demonstrated the effectiveness of the method and its superiority over the other three methods. The proposed method enables reliable process monitoring performance for a complete drilling cycle. However, in addition to changes in operating modes, formation changes can create uncertainties in process monitoring. As a promising future direction, it is necessary to investigate how to overcome the challenges brought by stratigraphic uncertainty, so as to meet the application requirements in different geological environments.

## REFERENCES

- [1] Y. Li, W. Cao, W. Hu, and M. Wu, "Abnormality detection for drilling processes based on Jensen-Shannon divergence and adaptive alarm limits," *IEEE Transactions on Industrial Informatics*, vol. 17, no. 9, pp. 6104–6113, 2021.

- [2] S. J. Hashemi, F. Khan, and S. Ahmed, "Multivariate probabilistic safety analysis of process facilities using the copula bayesian network model," *Computers & Chemical Engineering*, vol. 93, pp. 128–142, 2016.
- [3] W. Yu and C. Zhao, "Broad convolutional neural network based industrial process fault diagnosis with incremental learning capability," *IEEE Transactions on Industrial Electronics*, vol. 67, no. 6, pp. 5081–5091, 2020.
- [4] C. Gan, W.-H. Cao, L.-Z. Wang, K.-Z. Liu, and M. Wu, "An improved dynamic optimization control system for the drilling rate of penetration (rop) and its industrial application," *IEEE Transactions on Industrial Electronics*, vol. 70, no. 6, pp. 6201–6208, 2023.
- [5] W. Yu, C. Zhao, B. Huang, and M. Wu, "A robust dissimilarity distribution analytics with Laplace distribution for incipient fault detection," *IEEE Transactions on Industrial Electronics*, DOI 10.1109/TIE.2023.3239861, pp. 1–10, 2023.
- [6] J. Wang, S. Sun, Z. Wang, X. Zhou, and P. Gyasi, "Alarm dead-band design based on maximum amplitude deviations and bayesian estimation," *IEEE Transactions on Control Systems Technology*, DOI 10.1109/TCST.2023.3240020, pp. 1–8, 2023.
- [7] J. Wang, F. Yang, T. Chen, and S. L. Shah, "An overview of industrial alarm systems: Main causes for alarm overloading, research status, and open problems," *IEEE Transactions on Automation Science and Engineering*, vol. 13, no. 2, pp. 1045–1061, 2016.
- [8] Y. Han, J. Liu, F. Liu, and Z. Geng, "An intelligent moving window sparse principal component analysis-based case based reasoning for fault diagnosis: Case of the drilling process," *ISA Transactions*, doi:10.1016/j.isatra.2021.09.016, 2021.
- [9] S. Muojek, R. Venkatesan, and F. Khan, "Supervised data-driven approach to early kick detection during drilling operation," *Journal of Petroleum Science and Engineering*, vol. 192, p. 107324, 2020.
- [10] W. Yu, M. Wu, B. Huang, and C. Lu, "A generalized probabilistic monitoring model with both random and sequential data," *Automatica*, vol. 144, p. 110468, 2022.
- [11] S. Zhang, C. Zhao, and F. Gao, "Incipient fault detection for multiphase batch processes with limited batches," *IEEE Transactions on Control Systems Technology*, vol. 27, no. 1, pp. 103–117, 2019.
- [12] A. Willersrud, M. Blanke, L. Imslund, and A. Pavlov, "Drillstring washout diagnosis using friction estimation and statistical change detection," *IEEE Transactions on Control Systems Technology*, vol. 23, no. 5, pp. 1886–1900, Sep. 2015.
- [13] Y. Li, W. Cao, W. Hu, Y. Xiong, and M. Wu, "Incipient fault detection for geological drilling processes using multivariate generalized gaussian distributions and Kullback-Leibler divergence," *Control Engineering Practice*, vol. 117, p. 104937, 2021.
- [14] Y. Yuan, Q. Qu, W. Cao, and M. Wu, "Modeling for coke quality prediction using gaussian function and SGA," *Science China Information Sciences*, vol. 65, p. 119202, 2022.
- [15] C. Zhao, W. Wang, C. Tian, and Y. Sun, "Fine-scale modeling and monitoring of wide-range nonstationary batch processes with dynamic analytics," *IEEE Transactions on Industrial Electronics*, vol. 68, no. 9, pp. 8808–8818, 2021.
- [16] Z. Zhang, X. Lai, M. Wu, L. Chen, C. Lu, and S. Du, "Fault diagnosis based on feature clustering of time series data for loss and kick of drilling process," *Journal of Process Control*, vol. 102, pp. 24–33, 2021.
- [17] Z. Zhang, X. Lai, S. Du, W. Yu, and M. Wu, "Early warning of loss and kick for drilling process based on sparse autoencoder with multivariate time series," *IEEE Transactions on Industrial Informatics*, DOI 10.1109/TII.2023.3242772, pp. 1–11, 2023.
- [18] J. Hu, F. Khan, L. Zhang, and S. Tian, "Data-driven early warning model for screenout scenarios in shale gas fracturing operation," *Computers & Chemical Engineering*, vol. 143, p. 107116, 2020.
- [19] X. Zhang, L. Zhang, and J. Hu, "Real-time diagnosis and alarm of downhole incidents in the shale-gas well fracturing process," *Process Safety and Environmental Protection*, vol. 116, pp. 243–253, 2018.
- [20] X. Sun, B. Sun, S. Zhang, Z. Wang, Y. Gao, and H. Li, "A new pattern recognition model for gas kick diagnosis in deepwater drilling," *Journal of Petroleum Science and Engineering*, vol. 167, pp. 418–425, 2018.
- [21] Y. Li, W. Cao, W. Hu, and M. Wu, "Detection of downhole incidents for complex geological drilling processes using amplitude change detection and dynamic time warping," *Journal of Process Control*, vol. 102, pp. 44–53, 2021.
- [22] Y. Yu, J. Wang, and Z. Ouyang, "Designing dynamic alarm limits and adjusting manipulated variables for multivariate systems," *IEEE Transactions on Industrial Electronics*, vol. 67, no. 3, pp. 2314–2325, 2020.
- [23] D. J. Wheeler and D. S. Chambers, "Understanding statistical process control," *Knoxville*, 1992.
- [24] N. A. Adnan, I. Izadi, and T. Chen, "On expected detection delays for alarm systems with deadbands and delay-timers," *Journal of Process Control*, vol. 21, no. 9, pp. 1318–1331, 2011.
- [25] S. Du, M. Wu, L. Chen, K. Zhou, J. Hu, W. Cao, and W. Pedrycz, "A fuzzy control strategy of burn-through point based on the feature extraction of time-series trend for iron ore sintering process," *IEEE Transactions on Industrial Informatics*, vol. 16, no. 4, pp. 2357–2368, 2020.
- [26] H. Chen, B. Jiang, S. X. Ding, and B. Huang, "Data-driven fault diagnosis for traction systems in high-speed trains: A survey, challenges, and perspectives," *IEEE Transactions on Intelligent Transportation Systems*, vol. 23, no. 3, pp. 1700–1716, 2022.



**Yupeng Li** (Student Member, IEEE) received the B.S. degree in Automation, in 2017, from Northeast Forestry University, Harbin, China, and the Ph.D. degree in Control Science and Engineering from the School of Automation, China University of Geosciences, Wuhan, China in 2023.

He was a visiting Ph.D. student from 2021 to 2022 with the Department of Chemical and Biological Engineering, University of British Columbia, Vancouver, BC, Canada. His current research interests include process monitoring and fault detection.



**Weihua Cao** (Member, IEEE) received the B.S., M.S., and Ph.D. degrees in Engineering from Central South University, Changsha, China, in 1994, 1997, and 2007, respectively. From May 1997 to 2014, he was a faculty member with the School of Information Science and Engineering at Central South University, attaining the position of full professor. In 2014, he moved to the China University of Geosciences, Wuhan, China, where he is a professor with the School of Automation.

He was a visiting scholar with the Department of Electrical Engineering, Alberta University, Edmonton, Canada, from 2007 to 2008. His current research interests include intelligent control and process control.



**Bhushan Gopaluni** (Member, IEEE) is a Professor in the Department of Chemical and Biological Engineering and Associate Dean, Education and Professional Development in the Faculty of Applied Science at the University of British Columbia (UBC). He is currently an associate editor for *Journal of Process Control*, *Journal of The Franklin Institute*, and guest editor for *Process Control Special Series* in the *Canadian Journal of Chemical Engineering*.

He received a Ph.D. from the University of Alberta in 2003 and a Bachelor of Technology from the Indian Institute of Technology, Madras in 1997 both in the field of chemical engineering. He is one of the leading experts on data analytics for process industry and has authored over 110 refereed articles in reputed international Journals and conferences. His publications have been recognized through best paper awards and keynote presentations.

He is also the recipient of the prestigious Killam Teaching Prize and the Dean's service medal from the University of British Columbia.

**Wenkai Hu** (Member, IEEE) is currently a Professor with China University of Geosciences, Wuhan, China. He received the B.Eng. and M.Sc. degrees in Power and Mechanical Engineering from Wuhan University, Wuhan, China, in 2010 and 2012, respectively, and the Ph.D. degree in Electrical and Computer Engineering from the University of Alberta, Edmonton, Canada, in 2016.

He was a Post-Doctoral Fellow from October 2016 to September 2018, and a Research Associate from November 2018 to February 2019 at the University of Alberta. His research interests include advanced alarm monitoring, process control, and data mining for complex industrial processes.





**Chao Gan** (Member, IEEE) received his B.S. degree in Process Equipment and Control Engineering from Wuhan Polytechnic University, Wuhan, China in 2014, and the Ph.D. degree in Control Science and Engineering from the School of Automation, China University of Geosciences, Wuhan, China in 2019.

He was working with the China University of Geosciences, where he is currently an Associate Professor. His current research interests include data-driven modeling and intelligent optimization

for the drilling process.



**Min Wu** (Fellow, IEEE) received the B.S. and M.S. degrees in engineering from Central South University, Changsha, China, in 1983 and 1986, respectively, and the Ph.D. degree in engineering from the Tokyo Institute of Technology, Tokyo, Japan, in 1999.

He was a faculty member of the School of Information Science and Engineering at Central South University from 1986 to 2014, and was promoted to Professor in 1994. In 2014, he joined the China University of Geosciences,

Wuhan, China, where he is a professor in the School of Automation. He was a visiting scholar with the Department of Electrical Engineering, Tohoku University, Sendai, Japan, from 1989 to 1990, and a visiting research scholar with the Department of Control and Systems Engineering, Tokyo Institute of Technology, from 1996 to 1999. He was a visiting professor at the School of Mechanical, Materials, Manufacturing Engineering and Management, University of Nottingham, Nottingham, UK, from 2001 to 2002. His current research interests include robust control and its applications, process control, and intelligent control.

Dr. Wu is a Fellow of the IEEE and a Fellow of the Chinese Association of Automation. He received the IFAC Control Engineering Practice Prize Paper Award in 1999 (together with M. Nakano and J. She).